PROCEEDINGS OF SCIENCE

Sensitivity study of $\mu^+ \to e^+ a\gamma$ cLFV decay with the MEG II apparatus

Elia Giulio Grandoni[a,b,*] **for the MEG II collaboration**

[a] *INFN Sezione di Pisa,*
Largo B. Pontecorvo 3, 56127 Pisa, Italy
[b] *Dipartimento di Fisica dell'Universitá,*
Largo B. Pontecorvo 3, 56127 Pisa, Italy

E-mail: eliagiulio.grandoni@phd.unipi.it, elia.grandoni@pi.infn.it

We report on a study of the sensitivity of the MEG II apparatus in the search for the charged-lepton flavor-violating decay $\mu^+ \to e^+ a\gamma$, involving an axion-like particle in a V–A chirality configuration. While forbidden in the Standard Model, this decay is predicted in several Beyond Standard Model scenarios. We performed Monte Carlo simulations with GEANT4 and analyzed data using the ROOT framework. Our studies indicate that an optimized data taking configuration, using a low muon beam rate ($R_\mu \simeq 1 \times 10^6\,\mu$/s) and a low photon energy threshold (10 MeV), maximizes the experimental efficiency. Analyzing only the 2021 and 2022 binded datasets, corresponding to aproximately on six days of data taking, we show that MEG II can reach a sensitivity limit of $F_{V-A}^{95\%\mathrm{CL}} \geq 1.13 \times 10^9$ GeV, improving upon the 2015 TWIST result of $F_{V-A}^{95\%\mathrm{CL}} \geq 1.00 \times 10^9$ GeV. This study demonstrates the capability of MEG II to set world-leading constraints on this cLFV decay.

European Physical Society Conference on High Energy Physics,
Palais Du Pharo, Marseille, France,
07-11 July 2025

*Speaker

ISSN 1824-8039. Published by SISSA Medialab.

PoS(EPS-HEP2025)441

1. Physics Motivation

The Standard Model (SM) of particle physics presents many unanswered questions, such as the Flavour Puzzle. The SM features three generations of fermions connected by various accidental symmetries. In the case of spontaneous symmetry breaking, a set of Pseudo-Goldstone Bosons is expected to emerge as generators of the broken symmetries [1]. In the leptonic sector, these new bosons can couple non-diagonally across the three fermion generations, enabling charged Lepton Flavour Violating (cLFV) interactions. These bosons, known as Axion-Like Particles (ALPs), can arise in several theoretical frameworks, such as the Peccei-Quinn symmetry in Quantum Chromo Dynamics (QCD) [2]. ALPs are particularly interesting as they can have extremely light masses and long decay times, making them a compelling candidate for Dark Matter phenomena [3]. The Lepton-Flavour-Violating (LFV) vertex can be described by the following tree-level effective interaction [4]:

$$\mathcal{L}_{\text{eff}}^{\text{LFV}} \supset \frac{\partial_\mu a}{f_a} \overline{\mu} \gamma^\mu (C_{\mu e}^V - C_{\mu e}^A \gamma^5) e + \text{h.c.} \tag{1}$$

where $C_{\mu e}^{V(A)}$ is the coupling that controls the Vectorial (Axial) LFV interaction and f_a the BSM energy scale. Over the past years, several experiments have searched for processes involving ALPs, but no evidence has been found. The most stringent Upper Limit in flavour physics experiments on the constant f_a is set by the TWIST collaboration in 2015 [5] and the TRIUMPH experiment in 1986 [6] for different chiral configurations.

The decay process of interest for this study is $\mu^+ \to e^+ a\gamma$ in the $V - A$ chiral configuration for an ALP mass of 10 keV, which is formally realized by adding a Quantum Electro Dynamics (QED) vertex and fixing the chiral couplings to be $C_V = -C_A = 1$ in the Lagrangian in Eq. (1). This decay is referred to as the *Axion Radiative Muon Decay* (ARMD). The inclusion of a radiative correction is essential for detection with the MEG II apparatus, whose capabilities and performances are described in [7].

2. Single Event Sensitivity and Normalization

The Single Event Sensitivity (SES) is defined as the Branching Ratio corresponding to one signal event:

$$SES = \frac{1}{k}, \quad \text{with} \quad k = \frac{N_{ev}}{\mathcal{BR}}, \quad N_{ev} = 1 \quad \Longrightarrow \quad SES = \mathcal{BR}\,. \tag{2}$$

The normalization constant k depends on reconstruction efficiencies, geometrical acceptance, trigger efficiency, and data-taking time. Using GEANT4-based simulations [8] integrated into the MEG II framework, we model ARMD products to estimate these factors. The normalization for ARMD can be related to that of the MEG-like decay ($\mu^+ \to e^+\gamma$) normalization [9] through

$$k_{\text{ALP}} = F(E_\gamma) \cdot k_{\text{MEG II}}\,, \tag{3}$$

where $F(E_\gamma)$ encodes the photon-energy–dependent acceptance and efficiency corrections. To maximize the detection efficiency of the ARMD we need to lower the SW cut on the photon energy scale. Operating at high muon intensity poses challenges: relaxing the photon-energy and topology cuts exponentially increases the trigger rate. To keep it below the hardware limit of

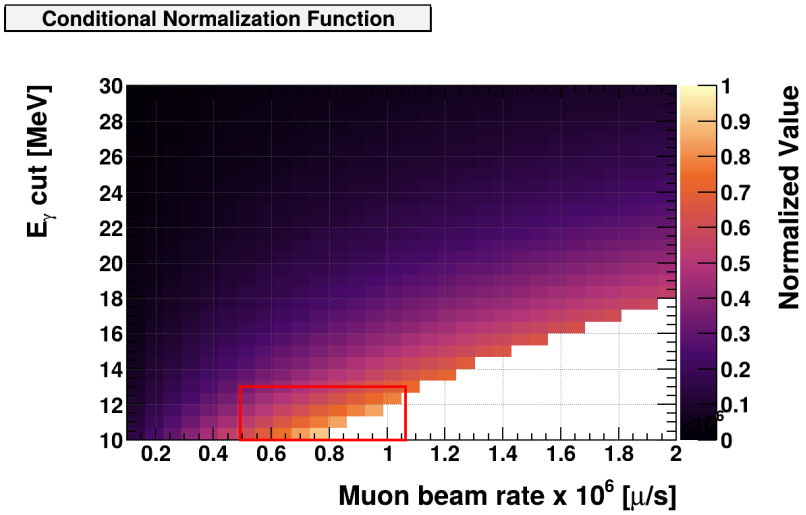

Figure 1: Behaviour of the conditional normalization (normalized to its maximum, z-COLZ axis) as a function of the photon energy cut and beam rate.

40–50 Hz, the beam intensity must be reduced dramatically from 4×10^7 to $\sim 1\times10^6\,\mu$/s. This also suppresses accidental backgrounds, scaling as R_μ^2, relative to Radiative Muon Decay, which scales only as R_μ [10]. Fig. 1 shows that the data taking configuration that optimizes the normalization constant is achieved at low photon-energy threshold ($E_\gamma^{\text{min}} \sim 10$ MeV) and reduced beam rate ($R_\mu \sim 0.5 \div 1 \times 10^6\ \mu/s$); this region is highlighted by the red box.

3. Analysis of the 2021 and 2022 data

For this analysis, we combine a likelihood-based method with a blinding-box approach. The blinding region is defined in two variables: the photon–positron time difference and the invariant missing mass squared of the visible ARMD decay products (M^2_{inv}). As 90% of the signal is expected to lie within the M^2_{inv} range of $[-85, 125]$ MeV^2, the data in this region were blinded. The time-difference distribution can be described by a constant component and a Gaussian term; the selection window on this variable is set to ±0.4 ns around the mean, corresponding to approximately 3σ of the Gaussian width. Figure 2 shows the scatter plot of the two variables for the 2021 and 2022 sideband data, while Figure 3 presents the corresponding single-variable distributions.

Normalization Estimate During the data taking, a trigger-level photon energy cut was applied to control the rate, introducing a smooth, error-function-like turn-on near the threshold due to detector response. To avoid this non-uniform efficiency, we impose analysis-level cuts: $E^{2021}_{\gamma,\text{cut}} = 22$ MeV, $E^{2022}_{\gamma,\text{cut}} = 26$ MeV. These cuts provide a stable photon spectrum but reduce ALP acceptance by shifting the positron distribution to lower energies, as most positrons are reconstructed above 40 MeV in MEG II. This cut modifies the proportionality factor in Eq. (3), yielding the ARMD normalization:

$$k^{\text{ALP}}_{2021} = (1.64 \pm 0.10) \times 10^7, \qquad k^{\text{ALP}}_{2022} = (1.06 \pm 0.07) \times 10^7. \tag{4}$$

PDFs Definitions and Sideband Fit The PDFs for the three event classes are defined using two complementary approaches. The ARMD and RMD PDFs are obtained from dedicated Monte

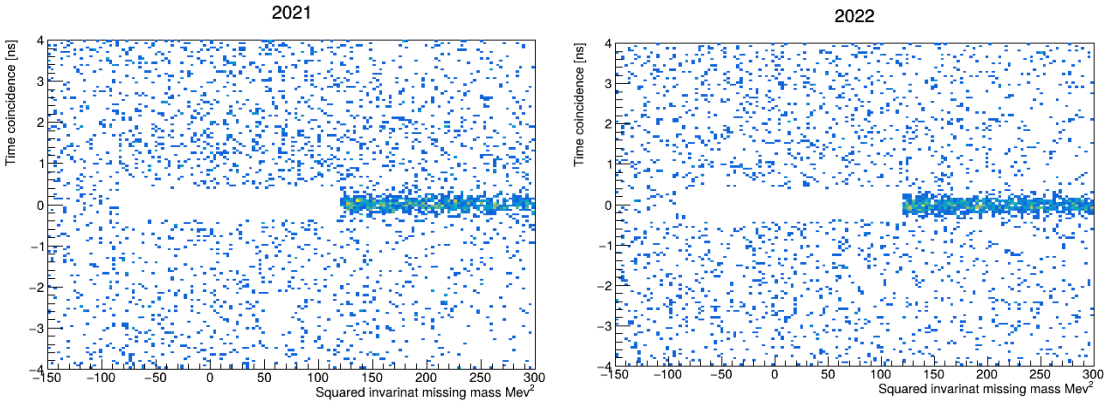

Figure 2: Two-dimensional distribution of time difference versus missing squared invariant mass in data for 2021 (left) and 2022 (right). In the plot we can distinguish the three main regions used in the analysis: the blinded signal region, the time-coincident sideband region for background estimation, and the non-coincident sideband region for modelling accidental backgrounds.

	Accidental	**RMD**
2021	272 ± 14	1563 ± 55
2022	242 ± 13	1764 ± 57

Table 1: Estimate of the number of background events from the two dimensional fit.

Carlo simulations, with a smearing procedure applied to match the detector resolutions observed in data with those extracted by the simulation. The accidental background PDF is instead extracted directly from data, using regions outside the time coincidence window. Each PDF is modelled with phenomenological analytical functions implemented in RooFit [11] for the M^2_{inv} (or $t_{e\gamma}$) variable: **ARMD** with a Double-Sided Crystal Ball function, **RMD** with a linear combination of two Landau functions (or a single Gaussian), and **Accidental background** with a linear combination of two Gaussians (or a constant PDF). The consistency between the chosen parametrizations and the observed data distributions is verified through a two-dimensional fit in the sideband region of the time-coincidence distribution. The projection of the fits for 2021 and 2022 are shown in Fig. 3, and the corresponding background yields are summarized in Tab. 1, this yield is used for the toy experiment construction in the sensitivity analysis.

Systematics Systematic uncertainties affect the measurement of the three main variables entering the analysis observable (M^2_{inv}). We adopt the nominal MEG II values for the positron energy and the positron–photon angle, and include a dedicated contribution for low-energy photons. The 1σ uncertainties are: $E_e^{\text{sys}} = 6$ keV, $\Theta_{e\gamma}^{\text{sys}} = 1$ mrad, $E_\gamma^{\text{sys}} = 0.5\% \cdot E_\gamma$. Their impact on the PDFs shapes is evaluated with MC simulations and incorporated into the final analysis.

Analysis Results To estimate the 95% CL Upper Limit on the number of signal events, we use the full frequentist Feldman-Cousins approach [12] using toy experiments with no signal: this leads to $N_{\text{ev}}^{95\%\text{CL}} \leq 60$ with a few percent worsening impact in case of systematics. The normalization from Eq. (4) can then be related to the decay constant $f_a = F_a\sqrt{2}$ (Eq. (1)) through $\mathcal{BR} = \frac{C \cdot \mathcal{I}}{f_a^2}$ (where

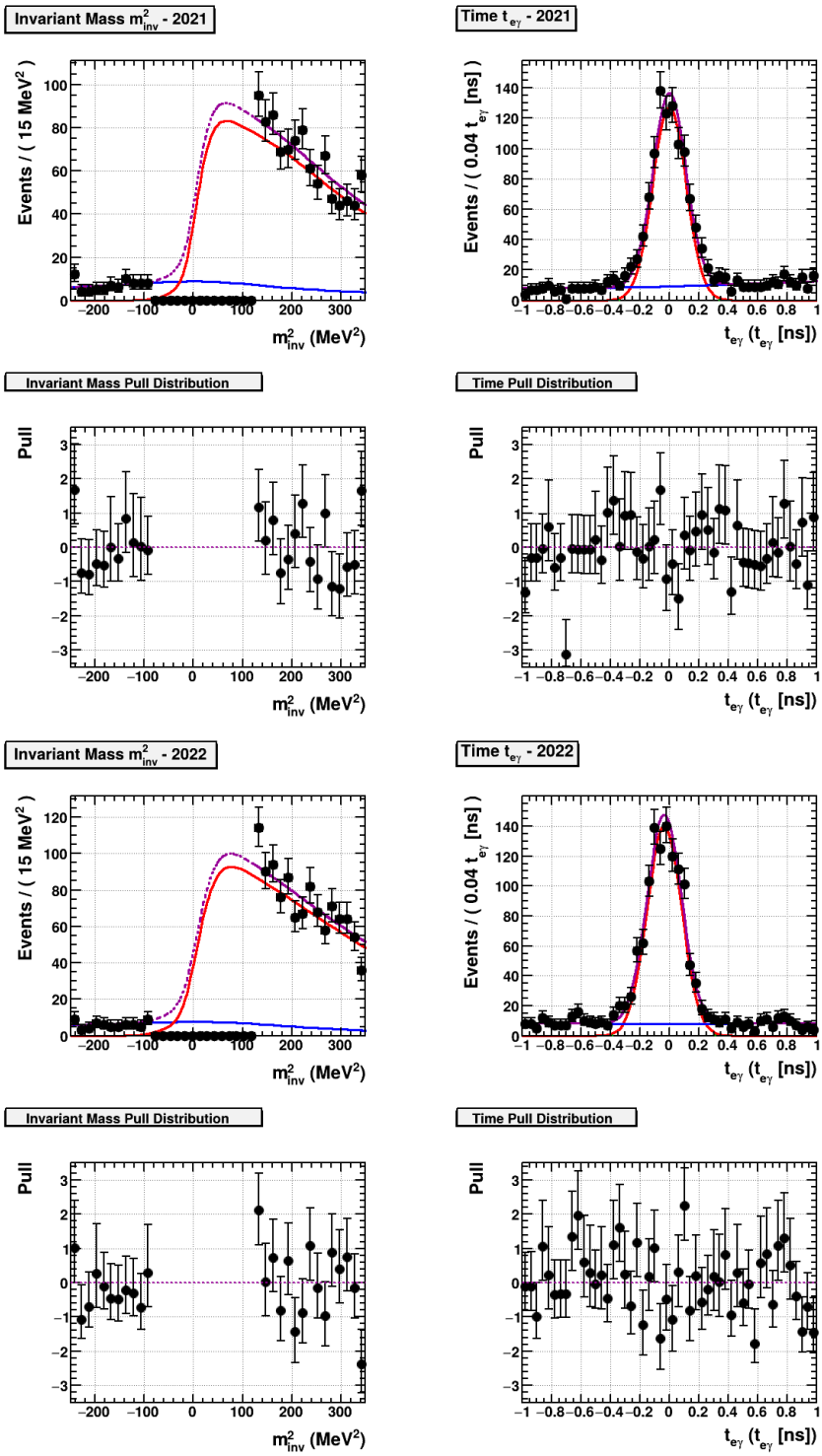

Figure 3: Comparison between 2021 (top) and 2022 (bottom) data and fitted PDFs for the 1D projection of the 2D fit. Top panels show the fitted PDF overlaid on the data for the two variables (invariant missing squared mass on the left and time difference on the right), while bottom panels show the pull distributions. In red the RMD background shape, in blue the accidental background shape, and in magenta their sum.

$C = 4.55 \times 10^{10}\,\mathrm{GeV}^2$ is a set of constants and $\mathcal{I} = 30.1$ the integral of the Branching Ratio on the adimensional phase space) , yielding

$$F_a^{95\%\mathrm{CL}} \geq \sqrt{\frac{2 \cdot C \cdot \mathcal{I} \cdot (k_{2021} + k_{2022})}{N_{\mathrm{ev}}^{95\%\mathrm{CL}}}} = 1.13 \times 10^9\,\mathrm{GeV}. \tag{5}$$

This improves the current best limit reported by the TWIST experiment [5] for the specific ALP mass and chiral configuration considered.

These results represent expected Monte Carlo sensitivity estimates. The unblinding of the 2021-2022 data is expected to take place before the end of 2025.

References

[1] S. Weinberg, "Approximate symmetries and pseudogoldstone bosons," *Phys. Rev. Lett.* **29** (1972), 1698–1701. doi:10.1103/PhysRevLett.29.1698

[2] R.D. Peccei and H.R. Quinn, "CP Conservation in the Presence of Pseudoparticles," *Phys. Rev. Lett.* **38**, 1440 (1977), doi:10.1103/PhysRevLett.38.1440.

[3] L. Calibbi, D. Redigolo, R. Ziegler and J. Zupan, "Looking forward to lepton-flavor-violating ALPs," *JHEP* **09**, 173 (2021), doi:10.1007/JHEP09(2021)173, arXiv:2006.04795 [hep-ph].

[4] Y. Jho, S. Knapen and D. Redigolo, "Lepton-flavor violating axions at MEG II," *JHEP* **10**, 029 (2022), doi:10.1007/JHEP10(2022)029, arXiv:2203.11222 [hep-ph].

[5] R. Bayes *et al.* [TWIST Collaboration], "Search for two body muon decay signals," *Phys. Rev. D* **91**, no.5, 052020 (2015), doi:10.1103/PhysRevD.91.052020, arXiv:1409.0638 [hep-ex].

[6] A. Jodidio *et al.* [TRIUMPH Collaboration], "Search for Right-Handed Currents in Muon Decay," *Phys. Rev. D* **34**, 1967 (1986), doi:10.1103/PhysRevD.34.1967. [Erratum: *Phys. Rev. D* **37**, 237 (1988)].

[7] K. Afanaciev *et al.* [MEG II Collaboration], "Operation and performance of the MEG II detector," *Eur. Phys. J. C* **84**, 190 (2024), doi:10.1140/epjc/s10052-024-12415-3, arXiv:2310.11902 [physics.ins-det].

[8] S. Agostinelli *et al.* [GEANT4 Collaboration], "GEANT4 – a simulation toolkit," *Nucl. Instrum. Meth. A* **506**, 250–303 (2003), doi:10.1016/S0168-9002(03)01368-8.

[9] A.M. Baldini *et al.* [MEG Collaboration], "Search for the lepton flavour violating decay $\mu^+ \to e^+ \gamma$ with the full dataset of the MEG experiment," *Eur. Phys. J. C* **76**, no.8, 434 (2016), doi:10.1140/epjc/s10052-016-4271-x, arXiv:1605.05081 [hep-ex].

[10] Y. Kuno and Y. Okada, "Muon decay and physics beyond the standard model," *Rev. Mod. Phys.* **73**, 151–202 (2001), doi:10.1103/RevModPhys.73.151, arXiv:hep-ph/9909265.

[11] W. Verkerke and D.P. Kirkby, "The RooFit toolkit for data modeling," *eConf* **C0303241**, MOLT007 (2003), doi:10.48550/arXiv.physics/0306116, arXiv:physics/0306116.

[12] G. J. Feldman and R. D. Cousins, "Unified approach to the classical statistical analysis of small signals," *Phys. Rev. D* **57**, 3873–3889 (1998), doi:10.1103/PhysRevD.57.3873.